Theoretical Study of Water Trimer

David J. Wales

Contribution from the University Chemical Laboratories, Lensfield Road, Cambridge CB2 1EW, U.K.

Received May 17, 1993•

Abstract: Geometry optimizations, rearrangement mechanisms, reaction pathways, spectral intensities, and tunneling splittings are reported for the water trimer at various levels of theory. Three of the four pathways which exist for a simple empirical rigid-molecule effective pair potential appear to be quite realistic, as evidenced by *ab initio* calculations of increasing quality up to DZP basis sets with correlation energy corrections from second-order Møller–Plesset theory. The spectroscopic consequences of the nonrigidity implied by the various rerrangement mechanisms are also considered; the pathways permit the interconversion within two subsets of the 96 permutationally distinct $(H_2O)_3$ clusters that arise when only O–H hydrogen bonds, as opposed to chemical bonds, may break. The associated tunneling spectra have also been calculated within a Hückel-type approximation, including estimates of the splittings associated with the different mechanisms. Quartet splittings are associated with both of the rearrangements that are likely to produce experimentally observable effects, and the order of magnitude predicted for the smaller of these is in reasonable agreement with experiment.

I. Introduction

Far-infrared vibration–rotation tunneling spectroscopy has recently yielded new insights into the hydrogen-bond tunneling processes in species such as ammonia and water dimers.[1,2] High-resolution spectroscopic techniques such as these provide a sensitive probe of intermolecular forces[3] including prototypical hydrogen-bonded systems. Inversion of spectroscopic data[4] can also produce detailed empirical potential energy surfaces which may be used to assess theoretical calculations and the adequacy of pairwise additivity, for example.

Clusters involving water molecules have been of particular interest, due to the unique significance of water as the universal solvent in which biochemical reactions occur. Pugliano and Saykally[5] have recently reported results for the perdeuterated water trimer, $(D_2O)_3$, and have provided a detailed group theoretical analysis of the tunneling spectra. They found that many vibration–rotation transitions are split into quartets and that tunneling occurs directly between left-handed and right-handed enantiomers.[5] They also speculated that such "transient chirality" might be exhibited by larger water clusters and have significant implications for reactions in aqueous media.

The aim of the present paper is to provide further theoretical developments against which to test these new experiments. A systematic study of the water trimer is therefore presented, including *ab initio* geometry optimizations of both minima and transition states using the standard Hartree–Fock SCF approach[6] with basis sets of increasing size up to DZP. For this largest basis set, calculations were also performed using second-order Møller–Plesset theory[7] to introduce correlation energy corrections. The results are all compared with those obtained from a simple empirical rigid-molecule effective pair potential, to provide some idea of the usefulness of such an approach. Three of the four rearrangements which exist for the latter potential are also found in the *ab initio* calculations. The infrared spectral intensities calculated for the intermolecular vibrations using basis sets of different sizes and the empirical potential also show some interesting features.

The rearrangement pathways having been studied in some detail, the implications for the tunneling splittings are considered. A simple computer program has been developed to analyze the topology of the effective molecular symmetry group in terms of the connectivity of the permutationally distinct minima on the potential energy surface. Estimates of the tunneling matrix element between minima that are linked by a given rearrangement are obtained, which, combined with the connectivity of the reaction graph, provide a quantitative prediction of the tunneling splittings within a Hückel-type approximation. The three different rearrangement mechanisms permit the interconversion of all the permutationally different water trimers within two disjoint sets, whose union is the complete set of structures that can be obtained without breaking any O–H chemical bonds. Quartet splitting patterns are found for both of the mechanisms which are likely to produce experimentally resolvable effects, and the estimated value for the smaller of these two splittings is in reasonable agreement with previously reported experimental results.[5]

II. Geometry Optimizations

This investigation begins with an approach which has now become standard in studies of atomic and molecular clusters bound by model empirical potentials and has been previously employed in investigations of the structure, dynamics, and rearrangement mechanisms of larger water clusters.[8] Local energy minima were found for $(H_2O)_3$ clusters bound by the T4 rigid-molecule effective pair potential by systematic quenching from a high-energy molecular dynamics (MD) trajectory. The T4 potential employed for this purpose includes a Lennard-Jones[9] interaction for each pair of oxygen atoms along with three point charges: two equal positive charges on the hydrogen atoms and a single negative charge which lies on the C_2 rotation axis displaced somewhat away from the oxygen atom toward the hydrogens. Examination of several parametrizations of this type[10] suggests that the T4

• Abstract published in *Advance ACS Abstracts*, October 1, 1993.

(1) Loeser, J. G.; Schuttenmaer, C. A.; Cohen, R. C.; Elrod, M. J.; Steyery, D. W.; Saykally, R. J.; Bumgarner, R. E.; Blake, G. A. *J. Chem. Phys.* **1992**, *97*, 4727.

(2) Pugliano, N.; Saykally, R. J. *J. Chem. Phys.* **1992**, *96*, 1832.

(3) Nelson, D. D.; Fraser, G. T.; Klemperer, W. *Science* **1987**, *238*, 1670. Saykally, R. J.; Blake, G. A. *Science* **1993**, *259*, 1570 and references therein.

(4) Cohen, R. C.; Saykally, R. J. *Annu. Rev. Phys. Chem.* **1991**, *42*, 369. Hutson, J. M. *Annu. Rev. Phys. Chem.* **1990**, *41*, 123. Hutson, J. M. *J. Phys. Chem.* **1992**, *96*, 4237.

(5) Pugliano, N.; Saykally, R. J. *Science* **1992**, *257*, 1937.

(6) See, for example: Szabo, A.; Ostlund, N. S. *Modern Quantum Chemistry*; McGraw-Hill: New York, 1989.

(7) Møller, C.; Plesset, M. S. *Phys. Rev.* **1934**, *46*, 618.

(8) Wales, D. J.; Ohmine, I. *J. Chem. Phys.* **1993**, *98*, 7245, 7257.

(9) Jones, J. E.; Ingham, A. E. *Proc. R. Soc. A* **1925**, *107*, 636.

(10) Jorgensen, W. L. *J. Am. Chem. Soc.* **1981**, *103*, 335; *J. Chem. Phys.* **1982**, *77*, 4156. Jorgensen, W. L.; Chandraesekhar, J.; Madura, J. W.; Impey, R. W.; Klein, M. L. *J. Chem. Phys.* **1983**, *79*, 926.

0002-7863/93/1515-11180$04.00/0

Table I. Parameters Used in the T4 Water Dimer Potential[10]

parameter	T4
OH distance/Å	0.9572
HOH angle/deg	104.52
$q_H/\|e\|$	0.520
$C_{12} \times 10^{-6}$/Å^{12} kJ mol^{-1}	2.510 400
C_6/Å^6 kJ mol^{-1}	2552.24
Δ/Å	0.15

form may give the best agreement with *ab initio* and theoretical results;[11] the values used are given in Table I. Explicitly, the total potential energy for a cluster of water molecules is given by

$$V = \sum_{\substack{i\in A,\ j\in B \\ A<B}} \left(\frac{q_i q_j e^2}{4\pi\epsilon_0 r_{ij}} + \frac{C_{12}}{r^{12}_{O_A O_B}} - \frac{C_6}{r^{6}_{O_A O_B}} \right)$$

where A and B label molecules, i and j are the charge sites, separated by distance r_{ij}, and $r_{O_AO_B}$ is the distance between the two oxygen atoms in molecules A and B. Each molecular geometry is fixed at the experimental structure, and the variable parameters are C_{12}, C_6, q_H (where $q_O = -2q_H$), and the displacement of the negative charge from the oxygen atom, denoted by Δ.

Stillinger and Weber[12,13] first introduced the idea of quenching to associate each point in nuclear configuration space with a local energy minimum ("inherent structure") on the potential energy surface (PES). In the present study, energy minimizations using a conjugate gradient method[14] were performed starting from MD configurations saved at intervals of 10^3 time steps along a trajectory of 10^6 time steps (0.4 ns in total) at a total energy of −39 kJ mol^{-1}. At this energy the cluster is highly nonrigid (the Lindemann δ, or relative root-mean-square internuclear distance,[8] is 0.15), and so we expect all the physically interesting regions of phase-space to be visited; energy was conserved to about one part in 10^3. Full details of such simulations, which were based upon the program of Tanaka and Ohmine,[15] may be found elsewhere.[8] We expect this procedure to reveal most of the important local minima on the PES; in this case the 10^3 quenches converged to either a single minimum (min) or (very rarely) a transition state (ts). This result emphasizes the need to inspect all the normal mode frequencies of geometries that have been produced by gradient optimizations.[16] Minima have only real frequencies, corresponding to positive eigenvalues of the mass-weighted second-derivative matrix, or Hessian. Transition states have precisely one imaginary frequency corresponding to a normal coordinate with negative curvature;[17] such stationary points are said to have Hessian index 1.

To search for further transition states and to perform all the *ab initio* stationary point and reaction path calculations, the Cerjan–Miller eigenvector-following approach was employed.[18] Numerous applications of this method have previously been reported for atomic and molecular clusters, where the first and second analytic derivatives of the energy are readily obtained.[19] The theory lying behind the specific step-taking method employed in this study has been discussed elsewhere.[20] All optimizations were conducted in Cartesian coordinates, as recommended by Baker and Hehre,[21] and implemented recently for calculations of the present sort.[22] The empirical rigid-molecule potential implies $6n$ degrees of freedom for a $(H_2O)_n$ cluster, $3n$ of which were taken to be center-of-mass coordinates, with the remaining $3n$ being Euler angles. The treatment of such systems has been discussed elsewhere.[8,22]

Transition-state searches were conducted starting from the first minimum in various states of contraction and following the "softest" five normal modes "uphill".[18,20,22] Four distinct transition states were found in all. To characterize the corresponding rearrangement pathways, each transition state geometry was perturbed by adding/subtracting a small displacement along the normal mode corresponding to the unique imaginary frequency. This procedure is described for the rigid-molecule calculations elsewhere;[8] for an assembly of atoms, the normal mode displacements are simply scaled by the square root of the reciprocal atomic mass. EF searches for minima were then initiated from the two perturbed geometries, one corresponding to each side of the reaction path.[23] Of the four transition states located, three are found to exist in the most accurate *ab initio* calculations performed in this study, and the full pathways corresponding to these structures were recalculated with DZP basis sets. The transition state which is not found in the latter calculations links the lowest energy minimum to a high-energy structure which is not a local minimum in most of the *ab initio* calculations. The others all mediate rearrangements of the global minimum, the cyclic trimer min1, which has alternating hydrogen bonds. The energies and point group symmetries of all the stationary points located with the T4 potential are listed in Table II. Further details and descriptions of the resulting mechanisms are given in section III.

The *ab initio* calculations were performed using the CADPAC program[24] to calculate the analytic first and second derivatives of the energy that are required for the present implementation of the eigenvector-following method.[20,22] Geometry optimizations were started from all six stationary points located for the T4 potential, searching for a minimum or a transition state, as appropriate. The basis sets employed were STO-3G (minimal basis, 21 functions), 4-31G (split-valence[25] basis, 39 functions), 4-31G* (split valence plus polarization;[26] the polarization functions consisted of a single set of p orbitals on each hydrogen (exponent 1.1) and a single set of six d orbitals on each oxygen (exponent 0.8), a total of 75 functions), and DZP (double-ζ[27] plus polarization: the polarization functions consisted of a single set of p orbitals on each hydrogen (exponent 1.0) and a single set of six d orbitals on each oxygen (exponent 0.9), a total of 78 functions). The global minimum was also reoptimized starting from the T4 geometry using DZP basis sets and including the second-order Møller–Plesset correlation energy correction.[7] However, as each calculation of the analytic energy derivatives in this case required nearly 1.5 Gbyte of disk space, the corresponding calculations for

(11) Tsai, C. J.; Jordan, K. D. *J. Chem. Phys.* **1991**, *95*, 3850.
(12) Stillinger, F. H.; Weber, T. A. *Kinam* **1981**, *3*, 159; *Phys. Rev. A* **1982**, *25*, 978; *J. Phys. Chem.* **1983**, *87*, 2833; *J. Chem. Phys.* **1984**, *81*, 5089, 5095; **1984**, *80*, 2742.
(13) Stillinger, F. H.; Weber, T. A. *Phys. Rev. A* **1983**, *28*, 2408.
(14) Press, W. H.; Flannery, B. P.; Teukolsky, S.; Vetterling, W. T. *Numerical Recipes*; Cambridge University Press: Cambridge, 1986.
(15) Tanaka, H.; Ohmine, I. *J. Chem. Phys.* **1989**, *91*, 6318. Ohmine, I.; Tanaka, H. *J. Chem. Phys.* **1990**, *93*, 8138.
(16) Uppenbrink, J.; Wales, D. J. *Chem. Phys. Lett.* **1992**, *190*, 447.
(17) Murrell, J. N.; Laidler, K. J. *Trans. Faraday Soc.* **1968**, *64*, 317.
(18) Cerjan, C. J.; Miller, W. H. *J. Chem. Phys.* **1981**, *75*, 2800. Simmons, J.; Jørgenson, P.; Taylor, H.; Ozment, J. *J. Phys. Chem.* **1983**, *87*, 2745. O'Neal, D.; Taylor, H.; Simmons, J. *J. Phys. Chem.* **1984**, *88*, 1510. Banerjee, A.; Adams, N.; Simmons, J.; Shepard, R. *J. Phys. Chem.* **1985**, *89*, 52. Baker, J. *J. Comput. Chem.* **1986**, *7*, 385; **1987**, *8*, 563.
(19) Wales, D. J. *J. Chem. Phys.* **1989**, *91*, 7002. Braier, P. A.; Berry, R. S.; Wales, D. J. *J. Chem. Phys.* **1990**, *93*, 8745. Wales, D. J. *Chem. Phys. Lett.* **1990**, *166*, 419. Davis, H. L. D.; Wales, D. J.; Berry, R. S. *J. Chem. Phys.* **1990**, *92*, 4308. Doye, J. P. K.; Wales, D. J. *J. Chem. Soc., Faraday Trans.* **1992**, *88*, 3295. Wales, D. J. *J. Am. Chem. Soc.* **1993**, *115*, 1557; **1990**, *112*, 7908. Wales, D. J.; Bone, R. G. A. *J. Am. Chem. Soc.* **1992**, *114*, 5399. Rafac, R.; Schiffer, J. P.; Hangst, J. S.; Dubin, D. H. E.; Wales, D. J. *Proc. Natl. Acad. Sci. U.S.A.* **1991**, *88*, 483. Wales, D. J.; Waterworth, M. *J. Chem. Soc., Faraday Trans.* **1992**, *88*, 3409. Wales, D. J.; Lee, A. M. *Phys. Rev. A* **1993**, *47*, 380.
(20) Wales, D. J. *J. Chem. Soc., Faraday Trans.* **1990**, *86*, 3505; **1992**, *88*, 653; *Mol. Phys.* **1991**, *74*, 1.
(21) Baker, J.; Hehre, W. J. *J. Comput. Chem.* **1991**, *12*, 606.
(22) Wales, D. J. *J. Chem. Soc., Faraday Trans.* **1993**, *89*, 1305.
(23) Fukui, K. *J. Phys. Chem.* **1970**, *74*, 4162; *Acc. Chem. Res.* **1981**, *14*, 363. Miller, W. H.; Handy, N. C.; Adams, J. E. *J. Chem. Phys. 72*, 99. Banerjee, A.; Adams, N. P. *Int. J. Quantum. Chem.* **1992**, *43*, 855.
(24) Amos, R. D.; Rice, J. E. *CADPAC: the Cambridge Analytic Derivatives Package, Issue 4.0*; Cambridge University: Cambridge, U.K., 1987.
(25) Francl, M. M.; Pietro, W. J.; Hehre, W. J.; Binkley, J. S.; Gordon, M. S.; DeFrees, D. J.; Pople, J. A. *J. Chem. Phys.* **1982**, *72*, 3654.
(26) Hariharan, P. C. *Theor. Chim. Acta.* **1973**, *28*, 213.
(27) Dunning, T. H. *J. Chem. Phys.* **1970**, *53*, 2823. Huzinaga, S. *J. Chem. Phys.* **1965**, *42*, 1293.

Table II. Energies, Hessian Indices, and Point Group Symmetries of the Stationary Points Located for the T4 Water Dimer Potential[10],[a]

	structure					
parameter	min1	min2	ts1	ts2	ts3	ts4
energy/kJ mol^{-1}	−70.025 243	−52.091 211	−69.968 051	−61.978 924	−53.677 195	−51.681 252
Hessian index	0	0	1	1	1	1
point group	C_1	C_1	C_1	C_s	C_s	C_1
barrier(s)/kJ mol^{-1}			0.057	8.046	16.348	18.344/0.410

[a] Minima and transition states have Hessian indices 0 and 1, respectively. Transition states ts1, ts2, and ts3 are for degenerate rearrangements of the global minimum, min1. ts4 is the transition state linking min1 to the high-energy minimum min2. The barriers for these rearrangements are also given.

Table III. Energies, Hessian Indices, and Point Group Symmetries of the Stationary Points Located in *ab Initio* Calculations for the Water Trimer[a]

	structure					
parameter	min1	min2	ts1	ts2	ts3	ts4
			STO-3G (time per step, 1.5[c] min)			
energy/h	−224.925 603	−224.921 271	−224.922 875	−224.922 875[d]	−224.919 143	−224.912 433
Hessian index	0	0	1	1	1	1
point group	C_1	C_1	C_1	C_1	C_1	C_1
barrier/kJ mol^{-1}			7.162		16.961	34.578/23.204
barrier[b]/kJ mol^{-1}			1.778		4.939	17.632/15.804
number of steps	12	81	10	32	23	12
NIIF	8	9	8	8	9	8
			4-31G (time per step, 5[c]/30[e] min)			
energy/h	−227.766 710		−227.766 689	−227.761 695	−227.755 032	
Hessian index	0		1	1	1	
point group	C_1		C_1	C_s	C_1	
barrier/kJ mol^{-1}			0.055	13.167	30.661	
barrier[b]/kJ mol^{-1}			<0	10.771	24.078	
number of steps	11	>50	9	6	9	>50
NIIF	3		3	3	3	
			4-31G* (time per step, 30[c]/15[f] min)			
energy/h	−227.886 531		−227.885 842	−227.883 623	−227.876 770[g]	
Hessian index	0		1	1	2	
point group	C_1		C_1	C_1	C_1	
barrier/kJ mol^{-1}			1.809	7.635	25.628	
barrier[b]/kJ mol^{-1}			0.064	4.830	16.339	
number of steps	9	>50	9	27	11	>50
NIIF	0		0	0	0	
			DZP[h] (time per step, 35[c]/21[f] min)			
energy/h	−228.164 825		−228.164 652	−228.162 203	−228.158 135	
Hessian index	0		1	1	1	
point group	C_1		C_1	C_1	C_1	
barrier/kJ mol^{-1}			0.454	6.884	17.110	
barrier[b]/kJ mol^{-1}			<0	4.562	10.319	
number of steps	9	>50	8	8	6	>50
NIIF	0		1	1	5	

[a] In most cases the optimizations were started from the converged T4 geometry. NIIF is the number of initial imaginary frequencies at the starting point. [b] Corrected for the zero-point energy calculated from the harmonic vibrational frequencies. [c] For a Silicon Graphics Indigo. [d] The corresponding structure in this case is a saddle of index 2; the optimization simply collapsed to give ts1. [e] For a Sun SPARCstation1+. [f] For a Convex 3840. [g] The corresponding structure in this case is a saddle of index 2. [h] These optimizations were started from the converged 4-31G* geometries.

the other structures were not attempted. It is perhaps worth noting that this is the only *ab initio* calculation that includes any of the dispersion energy which is introduced by the Lennard-Jones terms for the T4 potential. (**Note Added in Proof**: A DZP/MP optimization of the same structure has just been reported: Xantheas, S. S.; Dunning, T. H. *J. Chem. Phys.* **1993**, *98*, 8037. The geometry is in good agreement with that proposed by Pugliano and Saykally.[5] Some additional transition states have been located: Mó, O.; Yáñez, M.; Elguero, J. *J. Chem. Phys.* **1992**, *97*, 6628. However, these authors did not consider the rearrangement mechanisms and the barriers they found are probably higher than for ts2.) Each such step took about 2 h on a Convex 3840, and nine such steps were required for convergence. The initial geometry had four imaginary normal mode frequencies.

The *ab initio* results are summarized in Table III. In most of these calculations, a maximum step-length criterion of $0.15a_0$ was adopted to scale the eigenvector-following steps, if required. (It is convenient to use atomic units when discussing some of the present results. In this system, the hartree and bohr radius, a_0, are the units of energy and length, respectively, where 1 hartree = $4.359\,748 \times 10^{-18}$ J and $a_0 = 5.291\,772 \times 10^{-11}$ m.) It was necessary to increase the accuracy with which the various integrals were evaluated from the program defaults[24] to converge these optimizations efficiently. Optimizations were terminated when the root-mean-square gradient was less than 10^{-5} hartree a_0^{-1} and the maximum step length was less than 10^{-4} a_0. The six zero-normal mode frequencies were then never larger than about 2 cm^{-1} and were usually less than 1 cm^{-1}.

The results in Table III show that the topology of the PES is reasonably stable as the basis set is varied. min2 and ts4, which connects min2 to min1, only appear with the minimal STO-3G basis, and on two occasions we find that the structures corresponding to transition states for the T4 potentially actually have Hessian index 2 rather than 1. However, the optimizations conducted with the T4 potential are clearly useful starting points for *ab initio* studies and often appear to have qualitatively correct geometries. Furthermore, the quantum mechanical calculations may take several orders of magnitude more computer time. However, as all the structures were initially found in searches using the empirical potential, there may be concern that valid structures have been overlooked. On the other hand, the evidence

to date is that all the "true" minima and transition states (i.e., those which retain their character in more accurate calculations) are contained in the set of structures supported by the empirical potential; this certainly appears to be the case for the water pentamer, for which an analogous study is now in progress. Note that when the barriers are corrected for the zero-point vibrational energy, they are always decreased.

Of course, there have been a number of previous theoretical studies of small water clusters ranging from treatments using simple empirical potentials to *ab initio* calculations with larger basis sets than have been employed here. Various comparisons may be made with the present work. In particular, the approach of surveying the complex PES of a water cluster using an empirical potential and then performing selected quantum mechanical calculations was adopted in early studies by Clementi and co-workers.[28] This work succeeded in identifying low-energy minima which had not been previously considered in *ab initio* studies. In a later application, the method was extended to larger clusters[29] of up to eight molecules. Local energy minima in these studies were found by Monte Carlo methods, which have been combined with simulated annealing[30] in recent work by Tsai and Jordan[11] on water clusters of eight or more molecules. Cuboidal forms of $(H_2O)_8$ have attracted particular interest[11] and have been investigated with a wide range of empirical potentials.[31] A configuration interaction study of the water dimer[32] led to refinement of effective dimer potential functions, while other *ab initio* studies have often emphasized the division of the energy contributions into pair and many-body terms; Chalasiński *et al.* concluded that correlation effects do not contribute significantly to nonadditivity in the water trimer,[33] while van Duijneveldt *et al.* concluded that nonadditive effects are very important in determining the geometry and vibrational frequencies of the same species.[34] Both of these studies employ detailed counterpoise corrections to deal with basis set superposition errors and therefore do not include full geometry optimizations. A previous systematic investigation of the effect of basis set size upon the calculated stationary points of $(H_2O)_4$ concluded that a 4-31G* basis was sufficient to provide a reasonable description of the geometries.[35] A similar conclusion was reached by Herndon and Radhakrishnan in a comparison of geometries optimized for the empirical AM1 potential with *ab initio* calculations using 6-31G* basis sets.[36]

There have been various other studies which include either restricted or full geometry optimizations for $(H_2O)_3$ bound by different empirical potentials;[37,38] all of the most recent work essentially agrees that the global minimum is a cyclic trimer with alternating hydrogen bonds. Owicki *et al.*[38] also conducted transition-state searches using the Newton–Raphson method, and for $(H_2O)_3$ they identified ts1, in agreement with the present work. All of these structures are discussed in detail in the following section.

III. Rearrangement Mechanisms

We begin by discussing the minimum energy pathways found with the T4 potential and then consider how these change in the *ab initio* calculations. Where the details are different, the highest level *ab initio* calculation is likely to be the most realistic; however, the changes can be quite subtle, and it is interesting to see how well the empirical potential fares.

The important transition states characterized in section II, ts1–ts3, all mediate degenerate rearrangements of the global minimum, that is, they link minima which have the same geometry (or the mirror image) if atoms of the same element are not distinguished (Figure 1). In contrast, ts4 links the global minimum, with alternating hydrogen bonds, to min2, in which one molecule is a double hydrogen bond acceptor, another is a double donor, and only one is a donor and an acceptor (see Figure 1d).

Figure 1 was produced using Mathematica[40] with the hydrogen bonds specified by a distance cut-off (2.1 Å). Nine configurations are usually plotted along the rearrangement pathway. The first and last are the two minima in question, and the middle one is the transition state. The remaining six frames were selected at regular spacings along the two downhill paths, three on each side.

The rearrangement corresponding to Figure 1a is the "flipping" motion connecting enantiomeric structures referred to by Pugliano and Saykally,[5] for which a barrier of 2.5 kJ mol^{-1} was calculated by Owicki *et al.*[38] This estimate became negative[38] when a correction was made for the zero-point vibrational energy of $(H_2O)_3$ but remained positive (0.5 kJ mol^{-1}) for $(D_2O)_3$. The uncorrected barrier found for the T4 potential is 1 order of magnitude smaller, and very small values are also obtained from the *ab initio* calculations (Table III). Hence we expect this motion to be relatively facile and produce a large tunneling splitting, as discussed in section V.

The mechanism corresponding to ts2 (Figure 1b) has the next lowest barrier at all levels of calculations, and for the T4 potential includes a "C_2 rotation", as postulated by Pugliano and Saykally,[5] in which a single molecule effectively rotates about its own C_2 axis. However, this is accompanied by a "double flip", and the permutation-inversion operation represented by this process is different from that assumed by the above authors, as discussed in section V. As for ts1, this rearrangement connects enantiomeric structures. The barrier and relative motions involved suggest that tunneling splittings due to this mechanism may be significantly smaller than those due to ts1, and this view is supported by estimates of the relevant matrix elements in section V.

The pathway corresponding to ts3 is much longer than the others, and hence more frames are included in Figure 1c. Overall, this mechanism may also be described as a "C_2 rotation + double flip", as for ts2, and again links enantiomeric structures (section V). As expected, the barriers corresponding to ts3 are significantly larger than those for ts1 and ts2 at all levels of theory, and the very long reaction path is expected to produce relatively small tunneling splittings, as corroborated by the calculations in section V. Both ts2 and ts3 have C_s symmetry and differ mainly in the orientation of the end water molecule that lies in the plane.

The only donor–acceptor-exchange (DAE) mechanism[8] found in this study corresponds to ts4 (Figure 1d). As a result of a single DAE process, the global minimum is linked to the high-energy min2, which consists of one double donor, one double acceptor, and just one donor–acceptor molecule. Since this local minimum is only found for the T4 potential and in the minimal basis set calculations, it is not considered further in any detail.

All the above discussions are based upon pathways calculated for the T4 potential. For ts1–ts3, these were recalculated *ab initio* using DZP basis sets; the resulting paths were found to be very similar to those for T4, as shown in Figure 2. Once more,

(28) Popkie, H.; Kistenmacher, H.; Clementi, E. *J. Chem. Phys.* **1973**, *59*, 1325. Kistenmacher, H.; Lie, G. C.; Popkie, H.; Clementi, E. *J. Chem. Phys.* **1974**, *61*, 546.
(29) Kim, K. S.; Dupuis, M.; Lie, G. C.; Clementi, E. *Chem. Phys. Lett.* **1986**, *131*, 451.
(30) Kirkpatrick, P.; Gelatt, C. D.; Vecchi, M. P. *Science* **1983**, *220*, 671.
(31) Stillinger, F. H.; David, C. W. *J. Chem. Phys.* **1980**, *73*, 3384. Brink, G.; Glasser, L. *J. Phys. Chem.* **1984**, *88*, 3412.
(32) Matsuoka, O.; Clementi, E.; Yoshimine, M. *J. Chem. Phys.* **1976**, *64*, 1351.
(33) Chalasiński, G.; Szczęśniak, M. M.; Cieplak, P.; Scheiner, S. *J. Chem. Phys.* **1991**, *94*, 2873.
(34) van Duijneveldt, F. B.; Hartogh, M. de G.; van Duijneveldt-van de Rijdt, J. G. C. M. *Croat. Chem. Acta* **1992**, *65*, 1.
(35) Koehler, J. E. H.; Saenger, W.; Lesyng, B. *J. Comput. Chem.* **1987**, *8*, 1090.
(36) Herndon, W. C.; Radhakrishnan, T. P. *Chem. Phys. Lett.* **1988**, *148*, 492.
(37) Belford, D.; Campbell, E. S. *J. Chem. Phys.* **1987**, *86*, 7013.
(38) Owicki, J. C.; Shipman, L. L.; Scheraga, H. A. *J. Phys. Chem.* **1975**, *79*, 1794.
(39) Pechukas, P. *J. Chem. Phys.* **1976**, *64*, 1516.
(40) Mathematica 2.0 (Wolfram Research Inc.): Wolfram, S. *Mathematica*, 2nd ed.; Addison-Wesley: Redwood City, 1991.

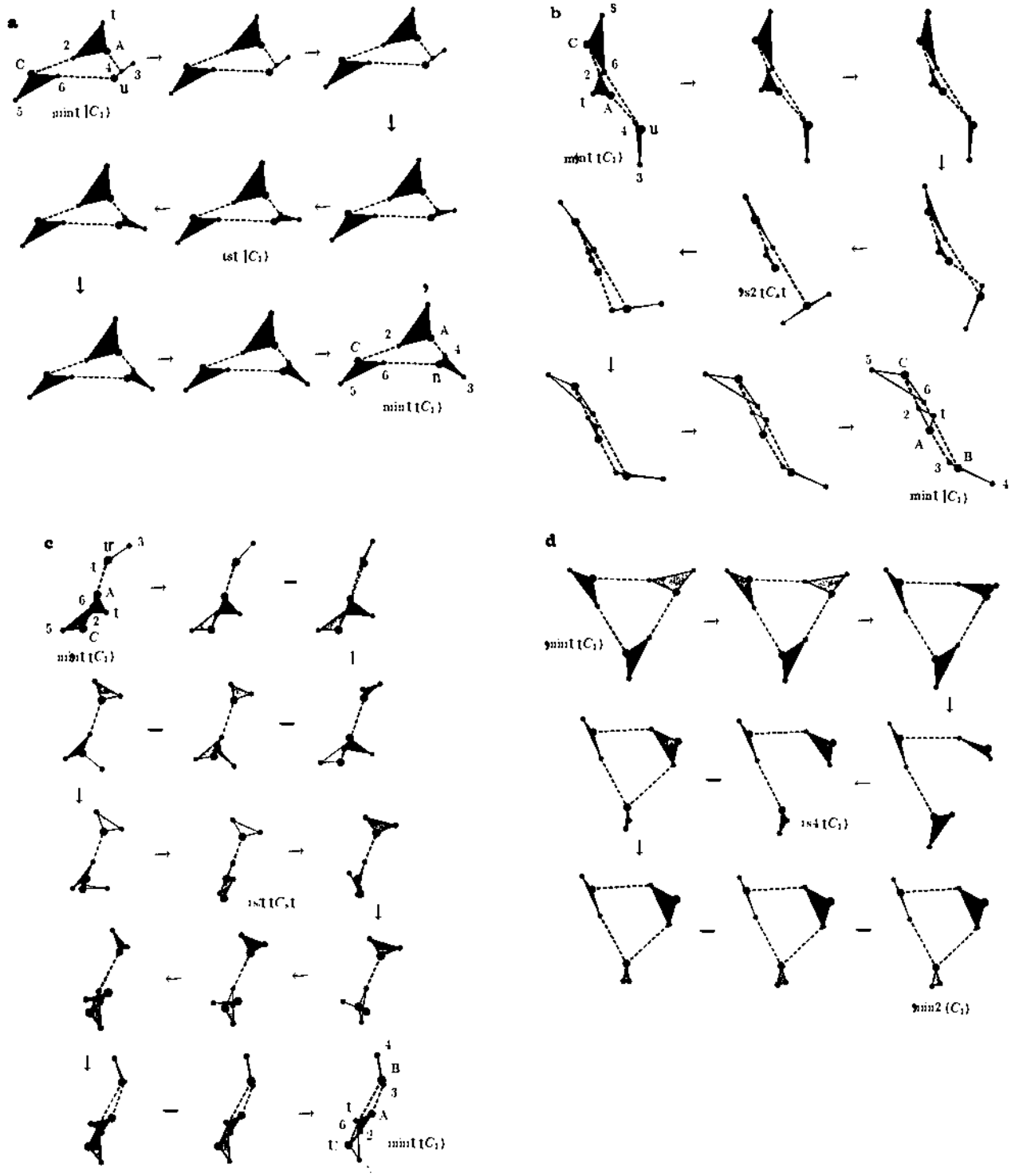

Figure 1. Rearrangements of $(H_2O)_3$ calculated with the T4 potential. (a) The mechanism corresponding to ts1, $(ABC)(135)(246)^*$; (b) ts2, $(34)^*$; (c) ts3 $(34)^*$; (d) ts4. Note that both ts2 and ts3 have a mirror plane which is not present anywhere else on the path.[39]

this shows that the simple empirical potential itself can provide valuable insights. However, there are some differences. For ts2 (Figure 2b) the "C_2" rotation is accompanied by a single rather than a double "flip". Furthermore, the *ab initio* rearrangement does not link enantiomeric structures and leads to a different splitting pattern. Hence we cannot assume that if a classically determined transition state appears to be reproduced in *ab initio* calculations then the corresponding mechanisms will be exactly the same. However, this is still a good first approximation. Note that neither ts2 nor ts3 has any symmetry elements apart from the identity when calculated *ab initio* with DZP basis sets. However, the structures are otherwise very similar to their T4 counterparts.

It is possible to quantify certain aspects of the above minimum energy pathways to provide more insight into the nature of these rearrangements. The path length is defined as $S = \int ds$, the integrated arc length in 27-dimensional nuclear configuration space. S was calculated as a sum over the eigenvector-following steps:

$$S = \sum_{\text{steps}} \left(\sum_{i} \Delta Q_i^2 \right)^{1/2}$$

where ΔQ_i is the step for nuclear Cartesian coordinate Q_i and the

outer sum is over all the eigenvector-following steps. Both S and the Q_i have dimensions of length: no mass-weighting is involved. The values obtained for S when calculated from nine frames, as used in Figure 2, were typically only 5–10% smaller than those obtained from the full path, and so the values quoted in Table IV are probably quite well converged.

The moment ratio of displacement has previously been used by Tanaka and Ohmine[15] in their discussion of rearrangements in bulk water. It is defined as[13]

$$\gamma = \frac{N\sum_i [Q_i(s) - Q_i(t)]^4}{(\sum_i [Q_i(s) - Q_i(t)]^2)^2}$$

where $Q_i(s)$ is the value of the nuclear Cartesian coordinate Q_i for minimum s, etc., and N is the number of atoms. Since the minimum energy pathways are calculated in Cartesian coordinates, with overall translation and rotation projected out for each step,[22] γ is simply calculated using the relative positions of the two minima at the ends of the path. Tanaka and Ohmine[15] used an average over molecules and found that similar indices were obtained for the displacements in Cartesian coordinates and for a center-of-mass, Euler angle description. γ may be viewed as a measure of the cooperativity involved in the rearrangement: if only a single atom moves (localized process), then $\gamma = N$, whereas if all atoms move through the same distance (cooperative process), then $\gamma = 1$. Hence for the water trimer we expect $1 \leq \gamma \leq 9$. Tanaka and Ohmine[15] have also found that the distance in nuclear configuration space, D, between minima s and t can be useful in discovering when major geometrical transformations have occurred:

$$D = (\sum_i (Q_i(s) - Q_i(t))^2)^{1/2}$$

The three quantities s, γ, and D, along with the total number of eigenvector-following steps, are tabulated in Table IV for the reaction pathways calculated with the T4 potential and *ab initio* using DZP basis sets. The values for the two sets of calculations are quite similar: S and D are always larger for the T4 potential, while γ is also larger for ts1 and ts3. Note that the cooperativity index correlates well with expectations based upon Figures 1 and 2: the mechanism corresponding to ts1 (single molecule flip) is highly localized, while that corresponding to ts3 is the most delocalized or cooperative.

IV. Spectral Intensities

Only the spectral intensities for the global minimum geometry will be reported, as the transition states are not observable spectroscopically and the higher energy minimum does not exist at the more accurate levels of theory. In any case, the general trends reported below for min1 are also seen for the transition states.

The CADPAC package[24] was again used for the *ab initio* calculations of spectral intensities; all the frequencies reported are purely harmonic. For the T4 potential, the intensities were estimated by forming two-sided numerical derivatives of the dipole moment; analytic dipole derivatives were available in the *ab initio* calculations. The intensity, I_i, of a vibrational transition from the ground state, ψ'', to the state in which normal mode i is singly excited, ψ_i', is

$$I_i \propto |\langle\psi''|\hat{\mu}|\psi_i'\rangle|^2 = \left(\frac{\partial\hat{\mu}}{\partial X_i}\right)_e^2 |\langle\psi''|X_i|\psi_i'\rangle|^2$$

where X_i is a displacement along normal mode i, $\hat{\mu}$ is the dipole moment operator, and the derivative is to be evaluated at the equilibrium geometry. The derivatives were approximated for the T4 potential by evaluating the dipole moment for positive and negative displacements along the normal mode of magnitude 10^{-4} and summing the squares of the three components. The displacements were performed in center-of-mass, Euler angle

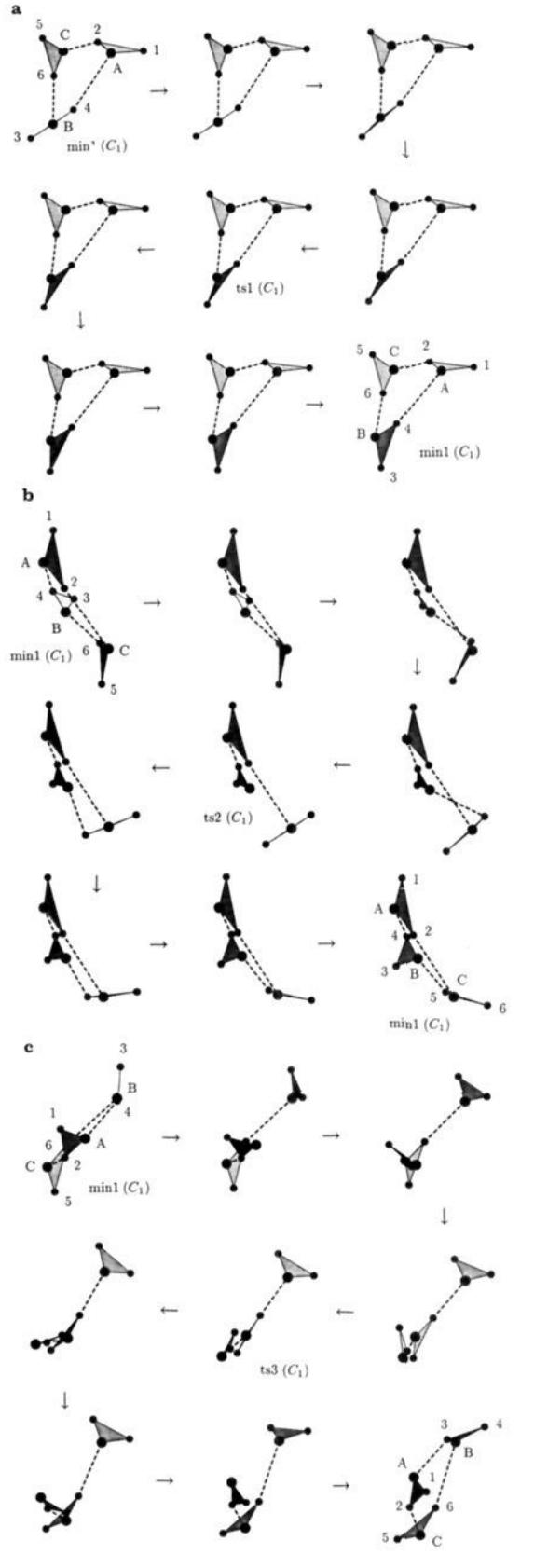

Figure 2. Rearrangements of $(H_2O)_3$ calculated *ab initio* with DZP basis sets for comparison with Figure 1. (a) ts1, the generator for the forward process is (ACB)(153)(264)*, the inverse of Figure 1a; (b) ts2, the generator for the forward process is (ACB)(164253); this is the pathway for the enantiomer of min1 as used in Figure 1 and part a of the present figure; (c) ts3, the generator for the forward process is (34)*; this is again the pathway for the enantiomer of min1 as for part (b).

Table IV. Characteristic Properties of the Reaction Paths Calculated with Both the T4 Potential and *ab Initio* Using DZP Basis Sets[a]

	pathway			
	ts1	ts2	ts3	ts4
	T4 Potential			
S/a_0	2.103	7.362	21.07	6.792
γ	6.540	2.579	2.604	2.781
D/a_0	1.882	4.800	4.590	4.977
γ_m/amu	1.450	3.592	4.117	3.379
γ_m'/amu	2.821	7.075	5.730	7.145
steps	26	30	82	36
	ab Initio DZP Basis			
S/a_0	2.053	5.988	17.10	
γ	6.452	3.085	2.310	
D/a_0	1.774	4.557	4.581	
γ_m/amu	3.021	3.057	15.563	
γ_m'/amu	4.308	5.966	18.682	
steps	32	53	81	

[a] S is the integrated path length, γ is the cooperativity index (1 for cooperative rearrangements, 9 for localized processes), D is the distance in nuclear configuration space between the two minima, γ_m is the effective mass for $(H_2O)_2$ defined in section V (γ_m' is for $(D_2O)_3$), and "steps" gives the total number of eigenvector-following steps in the path. A maximum step-length criterion was used in producing the pathways.[22]

coordinates,[8] and the stability of the derivative was checked for various displacements. Of course, there are only $6N-6$ vibrational normal modes for a set of N rigid bodies, which in this case correspond to the intermolecular modes. The resulting spectra are shown in Figure 3, where the integrated intensity for the T4 intermolecular modes has been set to the sum of the intensities of the corresponding low-frequency modes for the *ab initio* DZP/MP2 calculation. Of course, the results for the latter level of theory should be the most accurate, but it is interesting to compare them with the T4 potential and the lower level *ab initio* calculations. In fact, the reader may wish to examine Figure 3b before referring to the caption to discover which spectrum is which. A Lorentzian line shape was assumed,

$$L(\omega) = \frac{\hbar}{2\pi}\left[\frac{\Gamma}{(\Delta E - \hbar\omega)^2 + \Gamma^2/4}\right]$$

where Γ is related to the lifetime of the excited state, τ, by $\Gamma = \hbar/\tau$ (Γ = 10 cm^{-1} for Figure 3), ω is the frequency, and ΔE is the transition energy, and we sum over all the vibrations to get the total intensity. Both the line shape and the value of Γ were adopted purely to provide a convenient representation of the results. The vibrational frequencies for this minimum at all levels of theory are given in Table V.

Hopefully the reader will agree that the lower four spectra in Figure 3b are the most similar, and it is no surprise that the *ab initio* results with minimal STO-3G and split-valence 4-31G basis sets are somewhat different in appearance. However, the classical result for the T4 potential is actually qualitatively similar to those obtained for the larger basis sets, and hence such calculations may be useful for larger clusters, where reliable *ab initio* studies may not yet be possible. The vibration corresponding to the high-intensity feature at 733 cm^{-1} in the DZP/MP2 calculation is shown in Figure 4. This peak, which is identifiable in nearly all the calculations, corresponds to a motion consisting essentially of molecular librations, as expected for a high-frequency intermolecular mode.[15]

V. Tunneling Spectra

In this section we discuss the consequences of the rearrangements described above for the cluster energy levels and estimate the magnitudes of the expected tunneling splittings; more details

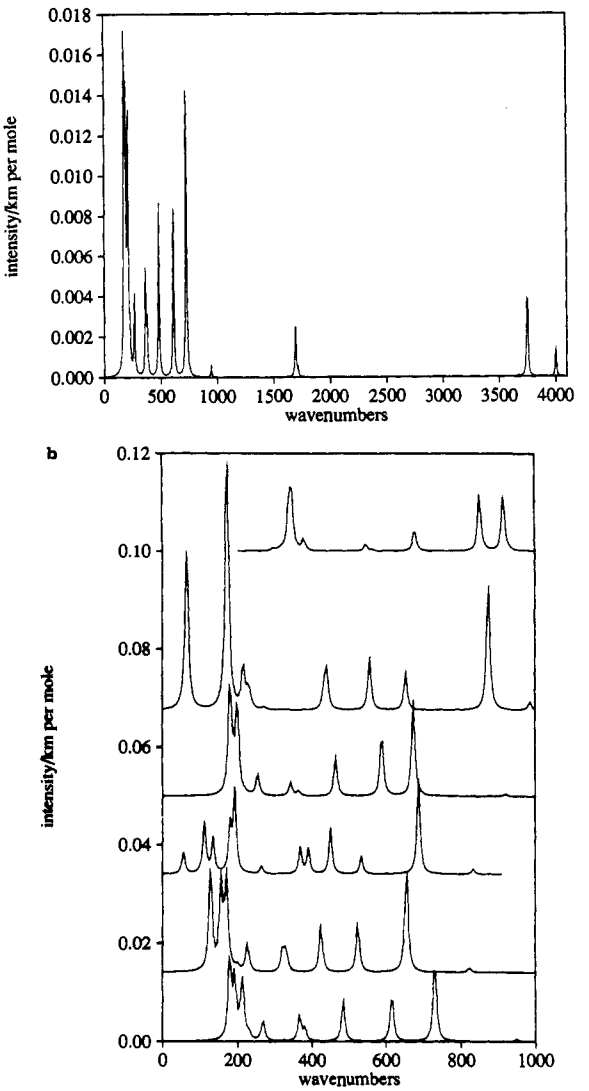

Figure 3. (a) Calculated DZP/MP2 spectral intensities for the global minimum of $(H_2O)_3$. (b) Enlargement of the region lying below 1000 cm^{-1} (essentially the intermolecular modes). From top to bottom: *ab initio*, STO-3G basis, 4-31G basis, 4-31G* basis, empirical T4 potential, *ab initio* DZP basis, and finally DZP basis with MP2 correlation correction. The spectra have been vertically displaced and given Lorentzian line shapes.

of these calculations are presented in a forthcoming report.[41] The terminology employed will be that used by Bone *et al.*[42] in their analysis of the acetylene trimer: a *structure* specifies a particular geometry which is associated with a number of *versions* that differ only in the arrangement of labeled atoms of the same element. The correct group in which to describe isomerization reactions is the effective molecular symmetry (MS) group.[43] This is a subgroup of the complete nuclear permutation-inversion (CNPI) group, whose operations include all permutations of labels of identical nuclei, the inversion of all coordinates through the origin of the laboratory-fixed axes (denoted E^*), and combinations of these operations. The operations of the CNPI group link all the versions of a given structure together. However, the MS group includes only "feasible" operations for which the activation energy barriers are not deemed to be prohibitive.[43]

For $(H_2O)_3$, the number of different versions is $2 \times 3! \times 6! = 8640$, and this is also the dimension of the CNPI group. However, if we include only versions in which the same hydrogen atoms are always bound by covalent bonds to the same oxygen atoms then

(41) Wales, D. J. *J. Am. Chem. Soc.*, companion paper in this issue.
(42) Bone, R. G. A.; Rowlands, T. W.; Handy, N. C.; Stone, A. J. *Mol. Phys.* **1991**, *72*, 33.
(43) Longuet-Higgins, H. C. *Mol. Phys.* **1963**, *6*, 445. Bunker, P. R. *Molecular Symmetry and Spectroscopy*; Academic Press: New York, 1979.

Table V. Harmonic Normal Mode Frequencies (cm^{-1}) of the $(H_2O)_3$ Global Minimum Calculated at Various Levels of Theory[a]

vibration	T4	STO-3G	4-31G	4-31G*	DZP	DZP/MP2
1	56	297	65	180	128	178
2	111	311	173	181	156	192
3	134	322	216	190	166	205
4	180	341	227	200	171	213
5	193	348	234	221	200	230
6	265	379	271	254	226	267
7	369	545	433	343	321	366
8	391	563	440	364	330	381
9	450	676	556	464	423	484
10	533	852	652	588	524	611
11	686	916	874	673	654	733
12	832	1290	985	919	823	948
13		2173	1772	1795	1769	1687
14		2174	1785	1804	1777	1694
15		2182	1829	1816	1796	1715
16		3981	3711	4004	4041	3673
17		4065	3776	4051	4078	3746
18		4072	3782	4054	4083	3754
19		4336	4083	4219	4249	4000
20		4353	4088	4222	4253	4003
21		4359	4094	4224	4255	4006

[a] The first column gives the results for the T4 empirical potential, and the remaining columns give the results for *ab initio* calculations with the specified basis sets.

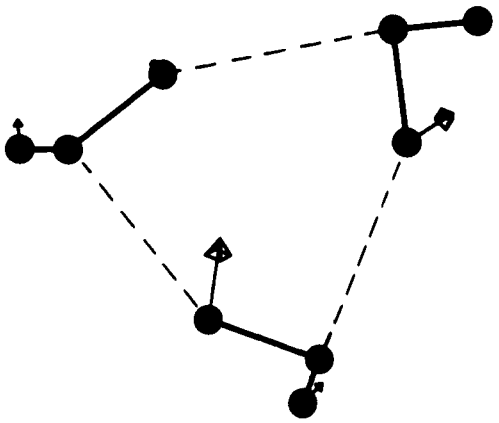

Figure 4. Appropriately scaled normal mode displacements for the 733 cm^{-1} vibration of min1 calculated at the DZP/MP2 level of theory. The vector field was plotted with Mathematica.[40]

we define 90 subgroups of the CNPI group of dimension $2 \times 3! \times (2!)^3 = 96$ each. Pugliano and Saykally[5] postulated that the feasible rearrangements of $(H_2O)_3$ are such as to produce an effective MS group of this order. We may now revise this conclusion in the light of the present calculations.

Two programs were written to assist in this process, as detailed elsewhere.[41] The first program takes as input the calculated barrier for a given degenerate rearrangement, the displacement between the two minima, D, and an effective mass, γ_m. The latter parameter, values for which are given in Table IV, is designed to account for the fact that some of the system may be relatively unaffected by the rearrangement. We take

$$\gamma_m = \frac{N\sum_i m_i[Q_i(s) - Q_i(t)]^2}{\gamma\sum_i[Q_i(s) - Q_i(t)]^2}$$

where γ was defined in section IV. Hence, if all the atoms move through the same distance, then γ_m is the total molecular mass; if only one atom moves, then γ_m is the mass of that atom. Note that γ_m is significantly larger in the *ab initio* calculations for ts1 and ts3, probably because the oxygen atoms move more, but is smaller for ts2, where the mechanism is actually slightly different. We require the tunneling matrix element, $\beta = \langle\psi_1|H|\psi_2\rangle$, where ψ_1 and ψ_2 are localized functions associated with the two minima

Table VI. Estimated Tunneling Matrix Elements β for Transition States ts1, ts2, and ts3 of the Water Trimer (cm^{-1})

	β_1	β_2	β_3
		T4 Potential	
$(H_2O)_3$	4.4	-9.9×10^{-6}	-1.6×10^{-9}
$(D_2O)_3$	4.1	-1.4×10^{-8}	-9.3×10^{-14}
		ab Initio DZP Basis	
$(H_2O)_3$	13	-4.4×10^{-5}	-4.2×10^{-20}
$(D_2O)_3$	8.7	-1.3×10^{-7}	-4.8×10^{-22}

that are linked by the rearrangement in question. β was calculated numerically taking $m = \gamma_m$ using Mathematica[40] by solving a model one-dimensional Schrödinger equation with a barrier width that depended upon the displacement, D. This approach is only intended to produce an order of magnitude estimate for the splitting, at best. Fortunately, the classification of the predicted splittings as "small", "medium", or "large" is relatively insensitive to details of the above procedure, and in particular to alternative estimates of the effective mass, which have been considered.

The second program takes as input sufficient permutation-inversion operations to generate the barrierless operations for the rigid molecule (in this case, just the identity, E), and then the generator operations and associated tunneling matrix elements (estimated in the first step) for the rearrangements. The program then works out the connectivity within a complete subgroup of the CNPI and constructs the appropriate secular matrix, whose eigenvalues give the energy levels and splitting pattern induced by the various rearrangement mechanisms.[44] If two versions are linked by a given rearrangement, then the corresponding secular matrix element is set to the estimated tunneling matrix element between them. If they are linked by more than one rearrangement, then the largest tunneling matrix element is assumed. As interactions between nonadjacent minima are neglected, this is a kind of Hückel approximation, though since the wave functions decay exponentially within classically forbidden regions, the basis of this approximation could be rather good. A full discussion is given in the accompanying report.[41]

First we need to deduce one of the feasible permutation-inversions corresponding to each of the rearrangements mediated by ts1, ts2, and ts3. For the pathways and labeling schemes of Figure 1 (T4 potential), the corresponding operations are (ABC)-(135)(246)*, (34)*, and (34)* again, using standard cycle notation (A is replaced by B is replaced by C, for example), where * denotes the inversion operation. Since all of these generators involve the inversion operation, they all interconvert enantiomeric structures. Three rearrangements of the "flip" type are needed to interconvert enantiomeric versions of the global minimum. The generators for ts2 and ts3 are the same, although the transition states are different (Figures 1b and 1c). Both have C_s symmetry, with the reflection operation also corresponding to the self-inverse operation (34)*. The generator for the rearrangement may be chosen to be the same operation in this case,[45] and the transition vector is antisymmetric with respect to this permutation-inversion. For ts2, the reaction path calculated by eigenvector-following in center-of-mass, Euler angle coordinates is unusually sensitive to the size of the displacement along the transition vector. For displacements of 1/50th and 1/100th of the renormalized, transformed eigenvector,[8] the water molecule lying in the mirror plane at the end of the chain returned to its original position instead of flipping. This result is obviously incorrect, because the motion is incompatible with the McIver-Stanton rules.[46] The correct answer was obtained with a displacement of 1/10th of the transformed eigenvector. For ts3, the same pathway was obtained with initial displacements of 1/100th and 1/10th the transformed eigenvector.

(44) Bone, R. G. A. Ph.D. Thesis, Cambridge University, 1992.
(45) Bone, R. G. A. *Chem. Phys. Lett.* **1992**, *193*, 557.
(46) McIver, J. W.; Stanton, R. E. *J. Am. Chem. Soc.* **1972**, *94*, 8618. Stanton, R. E.; McIver, J. W. *J. Am. Chem. Soc.* **1975**, *97*, 3632.

Table VII. Calculated Tunneling Splittings When Different Rearrangements Are Considered To Be Feasible in Addition to the Mechanism Corresponding to ts1[a]

T4 ts1 + ts2	*ab initio* ts1 + ts2	*ab initio* ts1 + ts2 + ts3
$2\beta_1 + \beta_2\ (A_1^+)$	$2\beta_1 + 2\beta_2\ (A_1^+)$	$2\beta_1 + 2\beta_2 + \beta_3\ (A_1^+)$
$2\beta_1 + {}^1/_3\beta_2\ (T_2^+)$	$2\beta_1 + {}^2/_3\beta_2\ (T_1^+)$	$2\beta_1 + {}^2/_3\beta_2 + {}^1/_3\beta_3\ (T_1^+)$
$2\beta_1 - {}^1/_3\beta_2\ (T_1^+)$	$2\beta_1 - {}^2/_3\beta_2\ (T_2^+)$	$2\beta_1 - {}^2/_3\beta_2 - {}^1/_3\beta_3\ (T_2^+)$
$2\beta_1 - \beta_2\ (A_2^+)$	$2\beta_1 - 2\beta_2\ (A_2^+)$	$2\beta_1 - 2\beta_2 - \beta_3\ (A_2^+)$
$\beta_1 + \beta_2\ (T_2^- \oplus E_1^-)$	$\beta_1 + {}^5/_3\beta_2 (T_2^-)$	$\beta_1 + {}^5/_3\beta_2 - {}^1/_3\beta_3\ (T_2^-)$
	$\beta_1 + \beta_2\ (T_1^- \oplus E_1^-)$	$\beta_1 + \beta_2 + \beta_3\ (E_1^-)$
$\beta_1 + {}^1/_3\beta_2\ (T_1^-)$		$\beta_1 + \beta_2 - \beta_3\ (T_1^-)$
$\beta_1 - {}^1/_3\beta_2\ (T_2^-)$	$\beta_1 - \beta_2\ (T_2^- \oplus E_2^-)$	$\beta_1 - \beta_2 + \beta_3\ (T_2^-)$
$\beta_1 - \beta_2\ (T_1^- \oplus E_2^-)$		$\beta_1 - \beta_2 - \beta_3\ (E_2^-)$
	$\beta_1 - {}^5/_3\beta_2\ (T_1^-)$	$\beta_1 - {}^5/_3\beta_2 + {}^1/_3\beta_3\ (T_1^-)$
$-\beta_1 + \beta_2\ (T_1^+ \oplus E_2^+)$	$-\beta_1 + {}^5/_3\beta_2\ (T_2^+)$	$-\beta_1 + {}^5/_3\beta_2 + {}^1/_3\beta_3\ (T_2^+)$
	$-\beta_1 + \beta_2\ (T_1^+ \oplus E_1^+)$	$-\beta_1 + \beta_2 + \beta_3\ (T_1^+)$
$-\beta_1 + {}^1/_3\beta_2\ (T_2^+)$		$-\beta_1 + \beta_2 - \beta_3\ (E_1^+)$
$-\beta_1 - {}^1/_3\beta_2\ (T_1^+)$	$-\beta_1 - \beta_2\ (T_2^+ \oplus E_2^+)$	$-\beta_1 - \beta_2 + \beta_3\ (E_2^+)$
$-\beta_1 - \beta_2\ (T_2^+ \oplus E_1^+)$		$-\beta_1 - \beta_2 - \beta_3\ (T_2^+)$
	$-\beta_1 - {}^5/_3\beta_2\ (T_1^+)$	$-\beta_1 - {}^5/_3\beta_2 - {}^1/_3\beta_3\ (T_1^+)$
$-2\beta_1 + \beta_2\ (A_2^-)$	$-2\beta_1 + 2\beta_2\ (A_1^-)$	$-2\beta_1 + 2\beta_2 - \beta_3\ (A_1^-)$
$-2\beta_1 + {}^1/_3\beta_2\ (T_2^-)$	$-2\beta_1 + {}^2/_3\beta_2\ (T_1^-)$	$-2\beta_1 + {}^2/_3\beta_2 - {}^1/_3\beta_3\ (T_1^-)$
$-2\beta_1 - {}^1/_3\beta_2\ (T_1^-)$	$-2\beta_1 - {}^2/_3\beta_2\ (T_2^-)$	$-2\beta_1 - {}^2/_3\beta_2 + {}^1/_3\beta_3\ (T_2^-)$
$-2\beta_1 - \beta_2\ (A_1^-)$	$-2\beta_1 - 2\beta_2\ (A_2^-)$	$-2\beta_1 - 2\beta_2 + \beta_3\ (A_2^-)$

[a] The form of these energy levels was deduced by inspection on varying β_1, β_2, and β_3 systematically.

C_s symmetry is only accurately retained in the *ab initio* calculations for ts2 with 4-31G basis sets; all the other transition states have C_1 symmetry and mediate asymmetric degenerate rearrangements.[47] For ts2, the generator is (ACB)(164253); this pathway was checked using displacements of 1/50th and 1/10th of the appropriate normalized eigenvector, which gave consistent results, the parameters in Table IV all changing by less than 0.1%. The other pathways were only calculated starting from geometries that had been subjected to the smaller of these displacements. The *ab initio* pathway for ts3 is equivalent to the T4 result, even though the transition state does not have C_s symmetry.

The generator for ts1 agrees with that used by Pugliano and Saykally,[5] but the others are different. The "clockwise-to-counterclockwise" mechanism hypothesized by Pugliano and Saykally[5] was not found in this study. The estimated tunneling matrix elements for all three mechanisms for both $(H_2O)_3$ and $(D_2O)_3$ are given in Table VI, where the T4 results are compared with those from the *ab initio* DZP calculations. The significance of these numbers is that the splittings may be divided into "large", "medium", and "small" for ts1, ts2, and ts3, respectively, and this is true for both the empirical potential and the *ab initio* results.

For ts1 alone, the MS group has six elements, and each minimum is connected to two others in sets of six; six different transition states are also associated with this chain, and there are 1440 different unlinked sets of this kind. The tunneling splittings corresponding to this mechanism are $2\beta_1(1)$, $\beta_1(2)$, $-\beta_1(2)$, and $-2\beta_1(1)$, where the degeneracies are in parentheses. These are the A_1, E_2, E_1, and A_2 levels described by Pugliano and Saykally,[5] respectively, where A_1 and E_1 have even parity under E^* and A_2 and E_2 have odd parity. The tunneling problem in this case is isomorphic to the simplest Hückel treatment of the π system of benzene; in each case we have six equivalent sites and one nearest-neighbor interaction matrix element. The parametrized secular determinant is therefore exactly the same. There is one complication which must, however, be mentioned here. As explained in the companion report,[41] it is convenient to present the tunneling levels in terms of a model secular determinant in which off-diagonal overlap is neglected and the diagonal Hamiltonian matrix elements are set to 0. This gives levels which can usually be written as straightforward multiples of β. There is often a simple linear relationship between these results and the roots of the full secular determinant, i.e., the energy differences are rescaled. However, for ts1 the motion is so facile that the full secular problem is always ill-defined, and in this case we simply quote the value of β. For the other mechanisms, the numerical β values are those obtained by rescaling after solving the full secular determinant.

For the other mechanisms, we must consider the T4 and *ab initio* cases separately. For T4, the generator is the same for ts2 and ts3 and on its own links isolated pairs of minima. When taken together with ts1, however, the size of the MS group increases to 48, i.e., half that of the largest MS group that is possible without breaking O–H covalent bonds; the new tunneling splittings are given in Table VII. The accidental degeneracies are typical of Hückel-type calculations.[48] Each minimum is now connected to three others, and the conservation of an energy pairing rule means that there are no odd-membered chains of minima, i.e., we expect to see Coulson–Rushbrooke-type pairing rules for the tunneling splittings of alternate reaction graphs, just as there are for alternate hydrocarbons.[49]

When we combined the generator for ts1 with the generator for the *ab initio* mechanism corresponding to ts2, the same group of order 48 results but with different splittings (Table VII). On including the generator corresponding to ts3, the size of the MS group is unchanged, but the accidental degeneracies are split (Table VII). Although a pairing relation is obeyed within each set of states that has the same coefficient of β_1, the pairing principle is now broken overall by the terms in β_3.

The largest MS group for both the T4 and *ab initio* pathways is the subgroup of G_{96} considered by Pugliano and Saykally[5] and analyzed by Balasubramanian and Dyke[50] which lacks the cycles of order 2 that would exchange pairs of water molecules. This group can be written as a direct product of $\{E,E^*\}$, a cyclic group of order 3 (corresponding to cyclic interchange of the three molecules), and the abelian group of order 8, which is itself the direct product of the three groups of order 2 that contain the permutations of hydrogen atoms attached to the same oxygen. It is not isomorphic to O_h, nor is it a direct factor of G_{96}; in fact, it is the same as the MS group deduced by Bone *et al.*[42] for the acetylene trimer if rotation of a single monomer is the only feasible rearrangement. The character table is given in Table VIII. If the 48 versions in any given set are represented as the vertices of a great rhombicuboctahedron (the 48 orbit of O_h), then the edges cannot be made to correspond to single step feasible operations.

The second computer program was extended to find the number of classes in the MS group and to determine the allowed electric

(47) Nourse, J. G. *J. Am. Chem. Soc.* **1980**, *102*, 4883.

(48) Hall, G. G. *Mol. Phys.* **1977**, *83*, 551.

(49) Coulson, C. A.; Rushbrooke, S. *Proc. Camb. Phil. Soc.* **1940**, *36*, 193.

(50) Balasubramanian, K.; Dyke, T. R. *J. Phys. Chem.* **1984**, *88*, 4688.

Table VIII. Character Tables for the Group of Order 48 Which is the Largest Molecular Symmetry Group Applicable to $(H_2O)_3$ When All the Rearrangements Calculated in This Study Are Feasible[a]

	1	4(ACB)	4(ABC)	4(ACB)	4(ABC)	3	3	1	1	4(ACB)	4(ABC)	4(ACB)	4(ABC)	3	3	1
	E	(164253)	(135246)	(153)(264)	(145)(236)	(12)	(12)(34)	(12)(34)(56)	E^*	(164253)*	(135246)*	(153)(264)*	(145)(236)*	(12)*	(12)(34)*	(12)(34)(56)*
A_1^+	1	1	1	1	1	1	1	1	1	1	1	1	1	1	1	1
A_1^-	1	1	1	1	1	1	1	1	1	1	1	1	1	1	1	1
A_2^+	1	−1	−1	1	1	−1	1	−1	1	−1	−1	1	1	−1	1	−1
A_2^-	1	−1	−1	1	1	−1	1	−1	1	−1	−1	1	1	−1	1	−1
E_1^+	1	ϵ	ϵ^*	ϵ	ϵ^*	−1	−1	1	1	ϵ	ϵ^*	ϵ	ϵ^*	−1	−1	1
E_1^+	1	ϵ^*	ϵ	ϵ^*	ϵ	−1	−1	1	1	ϵ^*	ϵ	ϵ^*	ϵ	−1	−1	1
E_2^+	1	$-\epsilon$	$-\epsilon^*$	ϵ	ϵ^*	1	1	1	1	$-\epsilon$	$-\epsilon^*$	ϵ	ϵ^*	1	1	1
E_2^+	1	$-\epsilon^*$	$-\epsilon$	ϵ^*	ϵ	1	1	1	1	$-\epsilon^*$	$-\epsilon$	ϵ^*	ϵ	1	1	1
E_1^-	1	ϵ	ϵ^*	$-\epsilon$	$-\epsilon^*$	−1	1	−1	1	ϵ	ϵ^*	$-\epsilon$	$-\epsilon^*$	1	−1	−1
E_1^-	1	ϵ^*	ϵ	$-\epsilon^*$	$-\epsilon$	−1	1	−1	1	ϵ^*	ϵ	$-\epsilon^*$	$-\epsilon$	1	−1	−1
E_2^-	1	$-\epsilon$	$-\epsilon^*$	$-\epsilon$	$-\epsilon^*$	1	1	1	−1	$-\epsilon$	$-\epsilon^*$	$-\epsilon$	$-\epsilon^*$	−1	1	−1
E_2^-	1	$-\epsilon^*$	$-\epsilon$	$-\epsilon^*$	$-\epsilon$	1	1	1	−1	$-\epsilon^*$	$-\epsilon$	$-\epsilon^*$	$-\epsilon$	−1	1	−1
T_1^+	3	0	0	0	0	−1	−1	−3	3	0	0	0	0	−1	−1	3
T_2^+	3	0	0	0	0	−1	−1	3	3	0	0	0	0	−1	−1	3
T_1^-	3	0	0	0	0	1	−1	−3	−3	0	0	0	0	−1	1	3
T_2^-	3	0	0	0	0	−1	−1	3	−3	0	0	0	0	1	1	−3

[a] The number of operations in each class is given along with a representative member of that class. $\epsilon = \exp(i\pi/3)$.

dipole transitions within a single manifold of states. The selection rule may be summarized as $\Gamma^+ \leftrightarrow \Gamma^-$. When only ts1 is included, the predicted spectrum is a quartet with the components separated by $2\beta_1$, $4\beta_1$, and $2\beta_1$. However, this is unlikely to account for the spectrum presented by Pugliano and Saykally,[5] where the separation is only of order 10^{-4} cm^{-1}. Introducing the generator corresponding to ts2 for the T4 potential, each quartet is split into a regularly spaced quartet, and the separations in both cases are $4\beta_2/3$. A new triplet also appears with the same separations.

Taking the generator for the *ab initio* mechanism corresponding to ts2 along with ts1 gives a different picture, in which the transitions at $\pm 4\beta_1$ are not split, while the lines at $\pm 2\beta_1$ are split into triplets with separation $8\beta_2/3$. Two new quartets also appear, each with spacings β_2, $2\beta_2/3$, and β_2. Introducing the generator corresponding to ts3 produces further splittings, but the foregoing estimates suggest that β_3 is probably too small for these to be observable.

VI. Conclusions

Minimum energy reaction pathways have been studied for the water trimer using the T4 rigid-molecule effective pair potential and *ab initio* calculations at various levels of theory. Most of the results obtained for the empirical potential are qualitatively reproduced in the more accurate calculations, including the predicted spectral intensities for the intermolecular vibrational modes. This is probably a reflection of the fact that the electronic structure of this complex is reasonably well represented by a single electronic configuration. Hence, the T4 potential is clearly of some value in studies of water clusters, either to provide a first approximation to the various properties in question or to provide starting points for more rigorous calculations.

The tunneling splittings have also been investigated, using computer programs to estimate the magnitude of the tunneling matrix elements and to find the appropriate reaction graph and set up the corresponding secular matrix. Diagonalizing this matrix gives the splitting pattern within a Hückel-type approximation. The magnitude of the tunneling matrix elements is estimated by effectively mapping the many-dimensional potential energy surface onto a model one-dimensional problem, using only simple properties of the calculated reaction path and ignoring zero-point corrections. More accurate calculations of tunneling levels are certainly possible[51] but would be much more complicated to perform.

This analysis helps to clarify some aspects of the tunneling spectra reported by Pugliano and Saykally[5] but will not provide a definitive answer without detailed consideration of the vibration–rotation levels involved in the transitions and perhaps nuclear spin statistical weights.[50] Both the T4 potential and *ab initio* calculations with DZP basis sets identify three basic degenerate rearrangements of the global minimum, and these are associated with tunneling splittings that may be classified as "large", "medium", and "small". The facile rearrangement corresponds to a "flipping" motion[5] in which no hydrogen bonds are broken and is associated with a tunneling splitting that is isomorphic to the Hückel π system of benzene. Transitions between these levels would give regularly spaced quartets, in agreement with experiment.[5] However, the detailed mechanism for the transition state corresponding to the medium-size splittings is slightly different in the two different calculations, and this gives rise to somewhat different splitting patterns. Quartet patterns (regularly or nearly regularly spaced) occur in both cases, and the order of magnitude estimated for this tunneling matrix element suggests that it is this mechanism which produces the subspectra observed experimentally.[5] The splittings due to the final rearrangement are not expected to be observable.

(51) Bell, R. P. *The Tunnel Effect in Chemistry*; Chapman and Hall: New York, 1980. Bunker, P. R.; Carrington, T.; Gomez, P. C.; Marshall, M. D.; Kofranek, M.; Lischka, H.; Karpfen, A. *J. Chem. Phys.* **1989**, *91*, 5154. Jensen, P.; Bunker, P. R. *J. Chem. Phys.* **1990**, *93*, 6266. Bunker, P. R.; Jensen, P.; Karpfen, A.; Kofranek, M.; Lischka, H. *J. Chem. Phys.* **1990**, *92*, 7432.

It should not be difficult to test these theoretical results against the detailed experimental spectra and determine which mechanism associated with ts2 is correct, if either. It is, of course, still possible that another low-energy degenerate rearrangement may have been missed, perhaps corresponding to one originally proposed by Pugliano and Saykally,[5] and that further analysis will be needed.

Acknowledgment. The author is a Royal Society University Research Fellow. This project was suggested by a stimulating seminar given at the University of Cambridge in February 1993 by Prof. R. J. Saykally and was subsequently encouraged by Prof. N. C. Handy. Some of the calculations were made possible thanks to a grant of supercomputer time from the SERC.